HHS Public Access

Author manuscript

J Biol Inorg Chem. Author manuscript; available in PMC 2015 November 11.

Published in final edited form as:

J Biol Inorg Chem. 2014 August ; 19(6): 967–979. doi:10.1007/s00775-014-1133-6.

Synthesis, Characterization, and Evaluation of *cis*-Diphenyl Pyridineamine Platinum(II) Complexes as Potential Anti-Breast Cancer Agents

Jacqueline Gamboa Varela[#],
Department of Chemistry, The University of Texas at El Paso, El Paso, Texas, 79968, USA

Atasi De Chatterjee[#],
Department of Biological Sciences and Border Biomedical Research Center, The University of Texas at El Paso, El Paso, Texas, 79968, USA

Priscilla Guevara,
Department of Biological Sciences and Border Biomedical Research Center, The University of Texas at El Paso, El Paso, Texas, 79968, USA

Verenice Ramirez,
Department of Chemistry, The University of Texas at El Paso, El Paso, Texas, 79968, USA

Alejandro J. Metta-Magaña,
Department of Chemistry, The University of Texas at El Paso, El Paso, Texas, 79968, USA

Dino Villagrán,
Department of Chemistry, The University of Texas at El Paso, El Paso, Texas, 79968, USA

Armando Varela-Ramirez,
Department of Biological Sciences and Border Biomedical Research Center, The University of Texas at El Paso, El Paso, Texas, 79968, USA

Siddhartha Das, and
Department of Biological Sciences and Border Biomedical Research Center, The University of Texas at El Paso, El Paso, Texas, 79968, USA

Jose E. Nuñez
Department of Chemistry, The University of Texas at El Paso, El Paso, Texas, 79968, USA

[#] These authors contributed equally to this work.

Abstract

Although cisplatin is considered as an effective anti-cancer agent, it has shown limitations and may produce toxicity in patients. Therefore, we synthesized two *cis*-dichlorideplatinum(II)

jenunez3@utep.edu, fax: 915-747-5748.

Supporting Information. Crystallographic data for compound **13** reported in this paper has been deposited with the Cambridge Crystallographic Data Centre as supplementary publication no. CCDC 933735. Copies of the data can be obtained free of charge from the CCDC (12 Union Road, Cambridge CB2 1EZ, UK; tel: (+44) 1223-336-408; fax: (+44) 1223-336-003; deposit@ccdc.cam.ac.uk; website see link below. Nuclear magnetic resonance (NMR) (^{1}H and ^{13}C), infrared, and mass spectra of both complexes, along with ^{1}H NMR spectra of the free ligands is available free of charge via the Internet at http://pubs.acs.org.

compounds (**13** and **14**) composed of *meta*- and *para*-*N*,*N*-diphenyl pyridineamine ligands through a reaction of the amine precursors and $PtCl_2$ with respective yields of 16% and 47%. We hypothesized that compounds **13** and **14**, with lipophilic ligands, should transport efficiently in cancer cells and demonstrate more effectiveness than cisplatin. When tested for biological activity, compounds **13** and **14** were found to inhibit the growth of MCF 7 and MDA-MB-231 cells (IC_{50s} 1 ± 0.4 μM and 1 ± 0.2 μM for **13** and **14**, respectively, and IC_{50} 7.5 ± 1.3 μM for compound **13** and 1 ± 0.3 μM for compound **14**). Incidentally, these doses were found to be lower than cisplatin doses (IC_{50} 5 ± 0.7 μM for MCF 7 and 10 ± 1.1 μM for MDA-MB-231). Similar to cisplatin, **13** and **14** interacted with DNA and induced apoptosis. However, unlike cisplatin, they blocked the migration of MDA-MB-231 cells suggesting that in addition to apoptotic and DNA-binding capabilities, these compounds are useful in blocking the metastatic migration of breast cancer cells. To delineate the mechanism of action, computer-aided analyses (DFT calculations) were conducted for compound **13**. Results indicate that in vivo, the pyridineamine ligands are likely to dissociate from the complex, forming a platinum DNA adduct with anti-proliferative activity. These results suggest that complexes **13** and **14** hold promise as potential anti-cancer agents.

Keywords

cisplatin; breast cancer drugs; platinum(II) complexes; diphenyl pyridineamine; apoptosis

Introduction

Square planar platinum(II) complexes have been investigated in a wide range of areas, including solid-state molecular dynamics [1-3], photo- and electroluminescence [4-11], and charge-transfer polymers [12-14]. Since the discovery of anti-cancer activity by a variety of platinum complexes and, in particular, cisplatin **1** (Figure 1) [15-16], these types of compounds have been tested on a wide variety of cancer cells and tissues as potential cancer-treatment agents [17-25]. Cisplatin, which is widely used in cancer treatment, is restricted by its limited activity to a narrow range of tumors as well as by severe side effects, such as nephrotoxicity, neurotoxicity, and myelotoxicity [19]. Although treating cancer patients with cisplatin and a combination of other cancer drugs is popular and initially effective, the developed resistance of cancer cells to cisplatin makes this method inefficient [26]. Thus, there is an urgent need to develop effective anti-cancer drugs that will produce minimum side effects.

Among the various designs, metal complexes composed of aromatic appendages are reported to exhibit a dual-function mode of action in which DNA binding occurs through coordination between the metal center and the DNA base pairs, along with π-π aromatic intercalations between the double helix and the aromatic components of the drug [21-24]. Complexes composed of phenanthroline, such as 56MESS **2**, phenanthrenequinone **3**, and pyridin-2-yl-acetate **4**, Figure 1, are reported to function through an intercalation mechanism only; however, these are still potent against cancer cells as compared to their non-intercalating analogs [21,27]. Recently, *trans*-type complexes, such as **5a** and **5b** have also been reported; however, the activity of *trans*-analogs has been studied to a lesser extent [17,21]. Substituted diphenylethylenediamine complexes reported by Schonenberger have

also been studied, for which hydroxyl and fluoro substituted analog **6a** exhibited lesser activity than the less hindered fluoro substituted complex **6b**, for which the authors argue a hydrogen-bonding effect within the DNA and Pt complex adduct [28-34]. Monofunctional derivatives of cisplatin containing only one leaving group have also been explored as potential anti-cancer agents, **7a**–**7h**, Figure 1 [35], which are reported to bind to DNA in a monodentate fashion, unlike the mode of action reported for cisplatin, which forms links between adjacent guanosine residues in DNA [35].

These compounds were designed to establish a structure-activity relation (SAR) by varying the size of the pyridine ligand. However, no SAR could be established, because out of the complexes with the larger ligands, **7f-h**, only **7g** exhibited better activity (up to 40 times greater) than cisplatin, whereas complexes **7f** and **7h** demonstrated lesser activity. Of the complexes with smaller ligands, **7b** is undergoing clinical trials, but the remaining complexes containing small ligands have not demonstrated efficient applications as cancer agents [35]. On the other hand, pyriplatin (**7a**) has been proven to work efficiently against certain tumors in mice [36,37].

Other designs include asymmetric-cyclometalated diamine **8** and ammonia-pyridyl complex **9**, Figure 1 [38,39]. Complex **8** was reported to exhibit high-antitumor efficiency against cisplatin-resistant mouse sarcoma in 180 cell lines. As for complex **9**, substitution of one amine group by a heterocyclic ligand did not increase binding of the complex to DNA but instead lowered the activity of the compound for both sensitive and resistant cell lines. Interestingly, pyridineamine complexes analogous to those reported in this work (**10**–**12**) that do not containing phenyl substituents on the amine groups have also been reported. However, these complexes exhibit low activity against sarcoma 180 [25], which leads to an interesting comparison with the compounds reported in this work and the potential benefit of molecules containing flexible organic ligands in anti-tumor activity.

In this article, we report the synthesis and characterization of complexes **13** and **14**, Figure 2, composed of *N*,*N*-diphenyl pyridineamine ligands (**15** and **16**), and demonstrate their anti-proliferative effects on breast cancer cells. We anticipate that the lipophilicity of the aromatic ligands may enhance cell permeation, as has been reported for similar platinum complexes [21,25], leading to enhanced activity. The observed anti-proliferative effects of **13** and **14** against MCF 7 and MDA-MB-231 support this prediction by demonstrating improved activity when compared with cisplatin. The novelty of the compounds lies in the structure of the organic ligands, which, contrary to the majority of the aromatic ligands explored in this area, provide a flexible complex that is highly lipophilic—a characteristic that promotes cell permeation. Contrary to typical designs for anti-tumor drugs, computational work suggests that in these molecules, the pyridyl ligands are more labile than the chlorides by about 4.5 kcal/mol and therefore may exhibit a different mechanism of action than cisplatin.

Materials and methods

Materials

All materials were used as received, unless specified. [*para*-amino pyridine, 18-crown-6, platinum chloride (Sigma Aldrich), bromobenzene, copper iodide (Alfa Aesar), *meta*-amino pyridine (TCI America), hexanes (Macron Chemicals), diethyl ether, acetone, potassium carbonate (BDH), dichloromethane (EMD)]. Cisplatin (Strem Chemicals Inc., Newburyport, MA), propidium iodide (Beckman Coulter, Miami, FL), penicillin/streptomycin (Hyclone, Logan, UT), Roswell Park Memorial Institute medium (RPMI-1640) and Dulbecco's Modified Eagle Medium (DMEM) were purchased from Gibco Invitrogen, Carlsbad, CA, and fetal bovine serum from Atlanta Biologicals, Lawrence, GA. NucView 488 Caspase-3/7 substrate (Biotium, Hayward, CA), JC-1 fluorescent dye (MitoProbe; Life Technologies, Grand Island, NY). Reaction solvents were dried over 4 Å molecular sieves (EMD) at least 24 h before use, or collected from a solvent purification system (MBRAUN). Reactions were monitored by silica gel thin layer chromatography using silica gel plates 60 F_{254} (EMD) and visualized under ultraviolet light (254 nm). Compound purifications were performed using 63-200 mesh 60 Å silica gel (EMD). Moisture sensitive reactions were carried out in oven-dried glassware under a nitrogen atmosphere, using standard Schlenk techniques. ^{1}H and ^{13}C NMR spectra were obtained with a JEOL 600 MHz spectrometer. Chemical shifts were recorded relative to residual proton or carbon resonances in deuterated solvents. Infrared (IR) spectra were obtained with a Perkin-Elmer FT-IR spectrum-100 spectrometer (equipped with ATR accessory) as neat solids. Melting points (Mp) were measured on a Mel-Temp melting point apparatus (1002D), and are uncorrected. Mass Spectra (MS) were acquired by electrospray ionization (ESI) measured on a JEOL AccuTOF JMS-T100LC ESI-MS spectrometer calibrated with PEG-600. Elemental analyses were performed by Galbraith Laboratories, Inc. (Knoxville, TN, USA). Sonicator (Model 150D, VWR), culture flasks (T75 vented cap, BD Biosciences, San Jose, CA), Cytomics FC 500 flow cytometer (Beckman Coulter). Data were recorded and analized with CXP software (Beckman Coulter). UV-light trans-illuminator (Alpha Innotech, San Leandro, CA).

X-ray diffraction

Crystals of compounds **13** suitable for x-ray diffraction were mounted on a glass fiber in a random orientation using paratone oil. The x-ray intensity data were collected with APEX2 [40] suited on a Bruker APEX CCD diffractometer with monochromatized MoK_{α} radiation (λ = 0.71073 Å) at room temperature for all of the crystals.

Synthesis of ligand 15

Meta-aminopyridine (1.00 g, 10.63 mmol) was dissolved in bromobenzene (25 mL) in the presence of CuI (0.30 g, 1.57 mmol), K_2CO_3 (2.80 g, 20.26 mmol), and 18-crown-6 (0.36 g, 1.36 mmol) under a nitrogen atmosphere, followed by heating to 150 °C for 12-20 h. The reaction mixture was cooled to room temperature, and worked up by addition of a saturated NH_4Cl solution. The aqueous layer was washed with diethyl ether (×3), dried over $MgSO_4$ and evaporated under reduced pressure to give a brown oily paste. The crude was purified by silica gel chromatography with 1:1 diethyl ether/hexanes as the eluent, to yield 1.41 g (54% yield) of a light, yellow powder. Ligand **16** was prepared under the same conditions as

15, with *para*-aminopyridine as the starting material, purified by silica gel chromatography with 100% diethyl ether as the eluent, yielding 2.12 g (81% yield) of a light, yellow powder.

Synthesis of *meta*- complex 13

Meta- ligand **15** (0.50 g, 2.03 mmol) and $PtCl_2$ (0.47 g, 1.77 mmol) were dissolved in benzene (50 mL) at 25 °C in a high-pressure vessel under a nitrogen atmosphere, followed by heating to 80 °C for 2 d. After allowing it to cool to room temperature, the yellowish precipitate was filtered and washed with CH_2Cl_2. Recrystallization of the filtered solid from a solution of CH_2Cl_2 and hexanes gave *cis*- isomer **13** (0.12 g, 16% yield) as a yellow powder. Mp = 285-289 °C (dec.) ^{1}H NMR (600 MHz, $CDCl_3$, TMS): δ 8.23 (d, *J* = 2.76 Hz, 2H), 8.14 (d, *J* = 5.46 Hz, 2H), 7.32-7.28 (overlapping dd and triplet, 10H), 7.16 (t, *J* = 7.56 Hz, 4H), 7.04 (dd, *J* = 5.58, 8.61 Hz, 2H), 6.98 (dd, *J* = 1.38, 8.22 Hz, 8H). ^{13}C NMR (150 MHz, $CDCl_3$, TMS): δ 146.3, 145.1, 144.7, 144.0, 130.3, 128.1, 125.8, 125.7, 125.5. FTIR (powder): 3059, 3034, 1588, 1563, 1480, 1452, 1426, 1333, 1300, 1270, 1189, 1171, 1153, 1112, 1074, 1026, 1002, 898, 881, 798, 756, 735, 690. HRMS calcd for $C_{34}H_{28}Cl_2N_4Pt$ (M^+) 757.1339; found (ESI): 781.1268 $(M+Na)^+$. Elemental analysis found: C, 53.06; H, 3.83; N, 7.30. Calcd for $C_{34}H_{28}N_4Cl_2Pt$: C, 53.83; H, 3.72; N, 7.39.

Synthesis of *para*- complex 14

Complex **14** was prepared under similar conditions as **13**, starting with *para*- ligand **16**. Purification by silica gel column chromatography with CH_2Cl_2 as the eluant, followed by addition of acetone gave **14** as a yellow powder (0.36 g, 47% yield). Mp = 299-300 °C (dec.) ^{1}H NMR (600 MHz, $CDCl_3$, TMS): δ 8.13 (d, *J* = 7.56 Hz, 4H), 7.39 (dd, *J* = 7.56, 8.22 Hz, 8H), 7.28 (t, *J* = 7.56 Hz, 4H), 7.18 (d, *J* = 7.56 Hz, 8H), 6.50 (d, *J* = 7.56 Hz, 4H). ^{13}C NMR (150 MHz, $CDCl_3$, TMS): δ 154.3, 151.8, 143.4, 130.4, 127.4, 127.2, 112.1. FTIR (powder): 3082, 3063, 1709, 1618, 1590, 1539, 1488, 1454, 1446, 1350, 1335, 1306, 1266, 1246, 1213, 1186, 1173, 1157, 1073, 1031, 904, 840, 822, 773, 756, 730, 700, 693. HRMS calcd for $C_{34}H_{28}Cl_2N_4Pt$ (M^+) 757.1339; found (ESI): 781.1299 $(M+Na)^+$. Elemental analysis found: C, 53.86; H, 4.00; N, 7.30. Calcd for $C_{34}H_{28}N_4Cl_2Pt$: C, 53.83; H, 3.72; N, 7.39.

Preparation of the platinum complexes solutions

Fresh stock solutions (10 mM) of compounds **13** and **14** were prepared in dimethyl sulfoxide (DMSO), followed by sonication in a water-bath sonicator for 1 min at room temperature, power level 9. Cisplatin was used as a positive control and was also prepared freshly in DMSO (stock concentration, 16.6 mM).

Culture of human breast cancer cells

Breast-cancer cells MCF 7 and MDA-MB-231 were cultured in RPMI-1640 and DMEM/Ham's F-12 media, supplemented with 10% fetal bovine serum and 1% penicillin/streptomycin [41]. The cancer cells were grown in a humidified atmosphere (95% air and 5% CO_2) until they reached ~90% confluency, then the confluent cells were trypsinized (0.25% Trypsin-EDTA, Hyclone), harvested by centrifugation, and grown in tissue-culture flasks.

Cell viability assay

Cells were harvested, plated on a 12-well plate (~1 × 10^5 cells per well) and incubated for 24 h at 37 °C. Various amounts (0, 1, 10, 20, and 50 μM) of compounds **13**, **14**, or cisplatin were added and the incubations were continued for an additional 24 h at 37 °C before harvesting the cells by trypsinization followed by centrifugation (× 3000 rpm, 5 min). The cells were counted under the microscope using haemocytometer to determine the viabilities of control and treated cells. To evaluate the effect of cisplatin, cells were treated for 24 h as reported by other investigators [42,43]. The effect of ligands **15** and **16** were also tested on the cell viability. For this, cells were plated and treated as described above. Different concentrations of ligand **15** (0.5, 1, and 1.5 μM for MCF 7 cells and 3.5, 7.5, and 10 μM for MDA-MB-231 cells) and ligand **16** (0.5, 1, and 1.5 μM for both MCF 7 and MDA-MB-231 cells) were used. The concentrations were chosen on the basis of the IC_{50s} for compounds **13** and **14**. The cells were incubated for 24 h at 37 °C and were counted under the microscope using haemocytometer.

Examination of phosphatidylserine (PS) externalization in cell membranes

Cells were plated in 24-well microplates at a density of 10,000 cells/well with 1 ml of growth media and incubated for 24 h. Next, MCF 7 cells were treated with 1 μM concentrations of compounds **13** or **14**; whereas MDA-MB-231 cells were treated with 7.5 μM and 1 μM concentrations of compounds **13** and **14**, respectively. Cisplatin was added at 5 μM concentration to MCF 7 and at 10 μM concentration to MDA-MB-231 cells. Cells were stained with fluorescein isothiocyanate (FITC)-conjugated annexin V and propidium iodide (PI) and analyzed by a Cytomics FC 500 flow cytometer [44]. For each sample, data from 10,000 events were recorded [45], and subsequently analyzed. Cells negative for both PI and annexin V were considered live cells; PI-negative, annexin V-positive staining cells were early apoptotic cells; PI-positive, annexin V-positive staining cells were cells in late stages of apoptosis; and PI-positive, annexin V-negative staining cells were necrotic [46-48]. The percentage of apoptotic cells was expressed as the sum of both early and late phases of apoptosis.

Analysis of mitochondrial membrane potential

The mitochondria membrane potential was analyzed by using 5,5',6,6'-tetrachloro-1,1',3,3'-tetraethylbenzimidazolylcarbocyanine iodide (JC-1), a lipophilic cationic aggregate-forming fluorescent dye, following the manufacturer's protocol, as a fluorescence probe. Human breast cancer cell lines were seeded into a 24-well plate at 100,000 cells/well in 1 ml culture media and allowed to attach overnight. The MCF 7 and MDA-MB-231 cells were treated with 1 μM and 7.5 μM concentrations of compound **13**, 1 μM concentrations of compound **14**, as well as 5 μM and 10 μM concentrations of cisplatin, respectively, and incubated for 8 h [49]. Subsequently, cells were stained with a 2 μM concentration of JC-1, following the manufacturer's protocol. Changes of the mitochondria ΔΨm were monitored in a live-cell modality via cytofluorimetric analysis. Polarized mitochondria allow JC-1 aggregation as indicated by the emission of red signals, whereas depolarized mitochondria allows the formation of JC-1 monomer, which can be detected by green signals. Cisplatin was included as a reference drug. A proton ionophore, carbonyl cyanide 3-chlorophenylhydrazone

(CCCP; 50 μM) was used as a positive control of mitochondrial ΔΨm depolarizer. In addition, solvent, 0.2% v/v DMSO, and untreated controls were concomitantly analyzed. Data acquisition and analysis was performed with CXP software.

Cell migration assay

Migration of breast cancer cells was tested as described by Cao et al. [50]. Briefly, ~1 X 10^6 cells were plated in each well of a 6-well plate and cultured as a monolayer to confluence overnight in RPMI-1640 and DMEM for MCF 7 and MDA-MB-231, respectively prior to serum starvation (5% Fetal Bovine Serum) for 24 h. Next day, the monolayers were wounded by scratching with a sterile 10 μl pipette tip [51] and treated with compounds **13**, **14**, or cisplatin for 24 h. The concentrations of the compounds used were their respective IC_{50} values. The images of the cells that had migrated between wounded regions were captured at 0 h and 24 h using a Nikon TMS microscope equipped with a Nikon F-601 camera. The number of cells that migrated into the wounded area was counted. All experiments were carried out in triplicate.

DNA mobility-shift assay

Interaction between DNA and any given molecule forming a DNA complex is investigated by monitoring the retardation of DNA migration using agarose gel electrophoresis [52]. Intercalation, or binding, of a chemical compound to DNA molecules results in decreased mobility of complexes after electrophoresis. Additionally, by using this approach, it is possible to evidence if there is any deleterious effect, causing direct plasmid DNA degradation or fragmentation by a given chemical compound. The reaction mixture in Phosphate Buffered Saline (PBS) (total volume: 10 μl) containing the platinum complexes (final concentration: 1 mM) and plasmid DNA (500 ng) were incubated for 30 min at 37 °C. The reaction was stopped by adding 2 μl of 6X gel loading buffer and placing the reaction tubes on ice. The samples were analyzed by using 1%-(w/v)-agarose-gels dissolved in TAE buffer (0.04 M Tris base, 0.04 M acetate, and 0.001 M ethylenediaminetetraacetic acid, EDTA). Ethidium bromide, a fluorescence agent, was used in the agarose gel during electrophoresis (0.5 μg/ml) for staining DNA. DNA was visualized under UV-light trans-illuminator. Cisplatin, and the widely used DNA intercalator, 4',6-diamidino-2-phenylindole (DAPI), were included as positive controls. Nystatin (1 mM) was included as a negative control.

Statistical analyses

All results were expressed as the mean ± SD, and statistical analysis was performed using Microsoft Excel (2007) software. Statistical analyses were performed using two-tailed Student's *t*-test. Differences were considered significant when $P < 0.05$.

Computational analyses

Density Functional-Theory (DFT) [53,54] calculations were performed with the hybrid Becke-3 [55-57] parameter exchange functional and the Lee–Yang–Parr [58] nonlocal correlation functional (B3LYP) as implemented in the Gaussian 09 program suite [59]. Double-ζ-quality basis sets (D95) [60], were used on nonmetal atoms (carbon, nitrogen, and

hydrogen). An Effective Core Potential (ECP) [61,62] representing the 1s2s2p3s3p3d core was used for the platinum atoms along with the associated double-ζ basis set (LANL2DZ). The convergence criterion for the self-consistent field cycles on all calculations was increased from the default value of 10^{-3} to 10^{-8}, in order to increase the statistical confidence and accuracy of the wavefunctions. Geometry optimization calculations were found to be minima in the potential energy surface as evidenced by the lack of imaginary vibrations in the frequency calculations. Transition state searches were performed using the Synchronous Transit-Guided Quasi-Newton (STQN) method [63] with the input of three initial geometries representing the reactants, products, and transition state guess (QST3) as implemented in Gaussian 09. All transition state geometries were identified as saddle-points in a potential energy surface by the location of one (and only one) imaginary frequency. The normal vibration mode of this imaginary frequency was germane to the studied mechanism of ligand substitution by a DMSO ligand. The transition state that describes the Substitution Nucleophilic bimolecular (SN2) displacement of chloride shows an imaginary mode of vibration 65*i* cm^{-1}, while the pyridineamine displacement mechanism showed a respective frequency of 89*i* cm^{-1}. All the calculations were performed on a full-atom model of **13** with no simplifications. A polarized continuum model [64,65] with DMSO solvent parameters, as implemented in the Gaussian 09 suite, was utilized on all calculations. All calculations were performed in a 44-processor Power Wolf PSSC supercomputer cluster running Linux Red Hat 4.1.2-54 located at the University of Texas at El Paso.

Results and Discussion

Synthesis of ligands

Known ligands **15** and **16** were prepared under Ullmann conditions in 53% and 81% yields, respectively, through a coupling reaction of the corresponding pyridineamines with bromobenzene by refluxing in the presence of CuI, K_2CO_3, and 18-crown-6 under a nitrogen atmosphere. A representative reaction for ligand **15** is depicted in Scheme 1 [66-73]. These are improved conditions for the synthesis of these ligands, which have been reported in 35% and 42% yields, respectively, as elimination products of 3-bromopyridines under strongly basic conditions [74].

Synthesis of complexes

Target complexes **13** and **14** were prepared following reported conditions for pyridine coordination complexes, as depicted in Scheme 1 for complex **13**, by dissolving the ligand in benzene, followed by addition of $PtCl_2$, and subsequently heating to 80 °C in a pressure vessel for 12-15 h [1-3,75]. Under these conditions, both *cis*- and *trans*- products are produced, however, due to the structural comparability to cisplatin, the current biological studies will only focus on the *cis*- analogs.

Both complexes were characterized by ^{1}H and ^{13}C nuclear magnetic resonance (NMR), infrared (IR) spectroscopy, and electrospray mass spectrometry (ES-MS). Complex **13** was further characterized by x-ray crystallography, as described below and in the Experimental Section. The complexes are robust, exhibiting no decomposition in solution for months, and melting points in the range of 285-300 °C with decomposition.

X-ray crystallography

Chiral complex *meta-cis* **13** crystallized from CH_2Cl_2 as a racemate in the centrosymmetric spatial group $P2_1/n$ with an inversion center that relates both isomers, Figure 3 (crystallographic parameters and selected bond lengths in Tables 1 and 2, respectively). The tilt of the pyridine groups with respect to the mean plane of the square planar system is 45.7° for the ring with N1, and 53.2° for that of N3. On the other hand, the dihedral angle between the two amino groups, N2 and N4, is 55.1° with respect to each ligand plane. Both ligands are planar at the central nitrogen, with dihedral angles of 31.3° (C2), 62.4° (C6), and 37.7° (C12) on the ligand containing N1. As for the ligand containing N3, the dihedral angles are 24.4° (C20), 59.7° (C24), and 49.9° (C30). This complex also exhibits H···Cl interactions between Cl1···H27 (2.89 Å), Cl2···H15 (2.87 Å) and Cl2···H34 (2.91 Å), as well as two-dimensional (2-D) sheets along with H···π interactions between H4 and C12 (2.86 Å), which contribute to the 2-D arrangement.

Attempts to grow x-ray quality crystals of *para-cis* **14** from CH_2Cl_2, $CHCl_3$, and mixtures of these solvents with hexanes, diethyl ether, and benzene, as well as diffusion methods using these solvents, produced very small crystals, from which the unit cell was solved, and determined to be equivalent to the unit cell of *meta-cis* **13**.

Compounds 13 and 14 inhibit the growth of breast cancer cells in culture

To evaluate potential biological activities, compounds **13** and **14** were tested on MCF 7 and MDA-MB-231 cells and their respective half-maximal cytotoxic concentrations (IC_{50s}) are shown in Table 3. While the IC_{50s} of compound **13** for MCF 7 and MDA-MB-231 are 1 ± 0.4 μM and 7.5 ± 1.3 μM, compound **14** inhibits MCF 7 at 1 ± 0.2 μM and MDA-MB-231 at 1 ± 0.3 μM concentration. Our results indicate that the activity of these two compounds is attributed to the flexible nature of the aromatic ligands. This conclusion is based on the low activity reported for analogous aminopyridine complexes of Pt(II) dichloride, **10–12** [25], Figure 1, which lack the two phenyl rings that complexes **13** and **14** possess at the central nitrogen atom of the ligands.

The activities of compounds **13** and **14** against MCF 7 and MDA-MB-231 cell lines were also compared with cisplatin [26, 42, 43, 76] and the results demonstrate that IC_{50s} of cisplatin against MCF 7 and MDA-MB-231 cells are 5 ± 0.7 μM and 10 ± 1.1 μM, respectively, which are higher than compounds **13** and **14** (Table 3). In a related experiment, we tested the effects of free ligands **15** and **16** (see the methods section) and no changes in viability were observed, indicating that anti-proliferative activities of compounds **13** and **14** are not due to their respective free ligands (data not shown).

Because many cytotoxic anti-cancer agents exert their effects by inducing apoptosis [77], we investigated whether compounds **13** and **14** also cause apoptosis in these two breast cancer cells. Therefore, control and Pt complexes-treated cells were labeled with Annexin V-FITC and PI and analyzed in live-cell modality by flow cytometry (Fig. 4), as described in the Experimental Section. Again, cisplatin was used as a positive control; since it has been reported to form DNA adducts that lead to cellular apoptosis [77].

We found that compounds **13** and **14** inhibit the growth of breast cancer cells by inducing apoptosis, results that are similar to cisplatin, although the concentration of cisplatin used is higher (IC_{50s} for cisplatin is 5 ± 0.7 μM for MCF 7 and 10 ± 1.1 μM against MDA-MB-231 cells) than compounds **13** and **14** (Fig.4). Interestingly, no significant increase in necrosis by these Pt compounds was noted. Figure 4b depicts the quantitative assessment of apoptosis presented in Fig. 4a, which indicate that all these compounds increase the number of apoptotic cells ~2 fold in MCF 7 and ~3–4 fold in MDA-MB-231 cells, compared with respective control cells (i.e. MCF 7 and MDA-MB-231). At this point it is not clear why MDA-MB-231 cells are more responsive to the Pt complexes than MCF 7 cells. These differences could be, however, due to the genetic and epigenetic makeup of the two different cell types.

Mitochondrial depolarization assay

Our next goal was to determine, at least in part, the mechanism by which these Pt complexes can induce apoptosis [78]. MDA-MB-231 cells were exposed for 8 h to compounds **13**, **14** and cisplatin, stained with JC-1 and monitored via flow cytometer in a live-cell fashion, as described in the Experimental Section. Findings displayed that mitochondrial membrane potential (Δψm) in MDA-MB-231 cells is altered by compound **13** as judged by an increase in the percentage of depolarized cells, demonstrative of mitochondrial ΔΨm perturbation (Fig. 5a and b). Also, a shift in the chromatic signal from red to green was detected in CCCP-treated cells, which were used as a positive control. In contrast, cells exposed to compound **14** and cisplatin mirrored the untreated cells, as evidenced by the absence of green signal, an indicative of unaltered Δψm. These results suggest that compound **13**, but not **14** and cisplatin, utilize the mitochondrial-dependent apoptotic intrinsic pathway to induce cell death in MDA-MB-231 cells (Fig. 5).

Wound-healing assays

Migration of cancer cells is associated with the activity of extracellular-matrix ligands and signals necessary for locomotion. Migration facilitates cancer cells by invading the surrounding tissue and colonizing to a new site to form a tumor [79,80]. Here, we asked if these Pt complexes blocked the migration of MDA-MB-231 cells. We used wound-healing assays, which are standard procedures in monitoring cell migration and angiogenesis in a laboratory setting [51]. The effect of compounds **13**, **14**, and cisplatin were examined on the migration of MDA-MB-231. Fig. 6a (photographs i–v) represents the migration of MDA-MB-231 cells across the wounded region after 0 and 24 h of incubation. Compounds **13** (photograph iii) and **14** (photograph iv) show significant inhibition (~65–70%) in migration compared to cisplatin (photograph v). As expected, poorly-migratory MCF 7 cells showed little or no migration across the wounded region under these experimental settings (not shown in Fig. 6a). The numbers of migrated cells in the wounded region were counted and are shown in Panel b along with the migratory values of MCF 7. Results show that both **13** and **14** are effective in blocking cell migration in culture, and are more potent than cisplatin.

Interaction with DNA

Usually, cytotoxic agents induce cell death either by interfering with the cell-cycle regulation or by inducing apoptosis [81]. Cumulative evidence suggests that cisplatin can cause cell death by first binding with DNA followed by activating the signaling pathways that lead to apoptosis [82]. Therefore, in the current study, we investigated if compounds **13** and **14** could interact with plasmid DNA forming heavier complexes, similar to cisplatin. The binding ability of these compounds was determined by mixing them with plasmid DNA followed by the mobility-shift assay on agarose gels. Compounds **13** and **14** showed shifts as compared with the control plasmid DNA alone and a cholesterol-binding drug, nystatin, which was used as a negative control (Figure S1 in Supporting Information). The shifts caused by compounds **13** and **14** are comparable with the changes (shifts) caused by DAPI, a DNA intercalating dye, and cisplatin, which binds to two consecutive guanine bases within DNA. Interestingly, it was observed that the plasmid DNA incubated with compound **14** consistently showed a band with lowfluorescence intensity, which could be due to the reason that compound **14** is already occupying to some extent the preferred interaction site of ethidium bromide; used to visualize plasmid DNA under UV light.

Computational modeling of the substitution reaction

^{1}H NMR experiments were carried out to determine complex stability in solution and to prove the proposed loss of ligands experimentally. However, after many days, the ^{1}H NMR spectra shows a mixture of signals representing the initial complex, the free ligand, as well as other signals that we interpret as dissociation products, making a straightforward analysis by ^{1}H NMR inconclusive. Therefore, we utilized Density Functional Theory calculations on an all-atom model of **13** in order to test the mechanistic pathway of substitution of the pyridineamine vs. chloride ligands bound to the platinum center by a DMSO-solvent molecule. Our calculations were based on a model that mimics the DMSO-solvent effect utilizing a polarized-continuum model (see computational details). In order to measure the activation barrier of SN2 ligand substitution, we performed a transition-state search for two potential mechanistic pathways: one in which a chloride ligand is displaced by an incoming DMSO molecule and another in which the pyridineamine ligand is displaced. We were able to find two appropriate transition-state geometries for each case that allowed us to measure the activation energy barrier of each mechanism. Fig. 7 shows the potential energy surface for both chloride and pyridineamine substitution. The geometry of the complex used to model the substitution reactions was based on the x-ray structural parameters of complex **13**. The first pathway described by SN2 substitution of the pyridineamine by a DMSO solvent molecule approaching the platinum center yields an activation barrier of 20.7 kcal/mol, whereas the chloride-leaving mechanism required 25.2 kcal/mol. This suggests that under the experimental conditions, pyridineamine substitution by DMSO from the platinum center is to some extent more favorable compared with loss of chlorides.

Conclusions

Development of new anti-cancer chemotherapies is a constant endeavor in the field of medicinal chemistry. In this context, the design and development of platinum-based complexes with anti-cancer activities (like cisplatin) are especially interesting and useful.

Therefore, in the current study, two *cis*-isomers of platinum(II) dichloride complexes composed of *meta*- and *para*-*N*,*N*-diphenyl pyridineamine derivatives (**13** and **14**) were prepared by initial synthesis of organic ligands **15** and **16** through copper-catalyzed reaction conditions, followed by coordination of the pyridine ligands with platinum dichloride. Furthermore, these complexes were found to be effective in blocking the growth and inducing apoptosis in MCF 7 and MDA-MB-231.

In addition, our findings demonstrate that compounds **13** and **14** also inhibit the migration of MDA-MB-231 cells possibly by affecting cytoskeletal organization membrane and vesicle flow, and cell polarity, as well as decreasing the levels of metabolic energy (ATP). The DNA-shift assay indicates that compounds **13** and **14** interact with DNA strands and produce platinum-DNA adducts, like cisplatin [82]. To the best of our knowledge, this is the first example of platinum(II) complexes composed of pyridine derivatives of triphenylamine that are tested for anti-cancer activity. Our results demonstrate a biological activity that is unique to complexes containing this type of pyridineamine derivatives, which provides these molecules with anti-cancer activity that is absent in structurally similar Pt(II) dichloride complexes, such as **10**–**12**, Figure 1 [25]. We speculate that both compounds (**13** and **14**) have potential as anti-breast cancer drugs and provide rational insight for its further evaluation in animal models.

Supplementary Material

Refer to Web version on PubMed Central for supplementary material.

Acknowledgment

The authors are thankful to the University of Texas at El Paso for financial support (Start-up funds and University Research Initiative). We also thank the National Science Foundation Grant CHE-0840525 (Mass Spectrometer), the Library, Equipment, Repair and Rehabilitation (LERR) State of Texas Funding (Nuclear Magnetic Resonance). Verenice Ramirez thanks the Minority Access to Research Careers (MARC) Program for financial support (2T34GM005048), and Jacqueline Gamboa Varela thanks the Campus Office of Undergraduate Research Initiatives (COURI) at UTEP for financial support via a 2011-2012 Research Stipend Award. Cell culture and flow cytometry analyses were carried out in Cytometry, Screening and Imaging Core Facility at the Border Biomedical Research Center (UTEP) supported by a grant (8G12MD007592) from the National Institute of Minority Health and Disparity of the National Institutes of Health (RCMI, NIMHD, NIH). Drs. Atasi De Chatterjee and Siddhartha Das were supported by a grant (R01AI096667) from the National Institutes of Allergy and Infectious Diseases (NIAID, NIH). The authors also thank Dr. Carl Dirk (UTEP) for helpful discussions and initial computational work. Galbraith Laboratories, Inc. for elemental analysis.

ABBREVIATIONS

IC_{50}	Inhibitory concentration 50%
CCCP	Carbonyl cyanide *m*-chlorophenyl hydrazone
DAPI	4',6-Diamidino-2-phenylindole
DFT	Density functional theory
DMSO	Dimethyl sulfoxide
Cisplatin	*Cis*-diammineplatinum dichloride

FITC	Fluorescein isothiocyanate
JC-1	5,5',6,6'-Tetrachloro-1,1',3,3'-tetraethylbenzimidazolylcarbocyanine iodide
PI	Propidium iodide
NMR	Nuclear magnetic resonance
IR	Infrared spectroscopy
FTIR	Fourier transform infrared
ESI-MS	Electrospray ionization-mass spectrometry
TMS	Tetramethyl silane
18-Crown-6	1,4,7,10,13,16-Hexaoxacyclooctadecane
EDTA	Ethylenediaminetetraacetic acid
ATP	Adenosine triphosphate
kcal/mol	kilocalorie per mole

REFERENCES

1. Zeits PD, Rachiero GP, Hampel F, Reibenspies JH, Gladysz JA. Organometallics. 2012; 31:2854–2877. doi: 10.1021/om201145x.
2. Nawara AJ, Shima T, Hampel F, Gladysz JA. J. Am. Chem. Soc. 2006; 128:4962–4963. doi: 10.1021/ja061044w. [PubMed: 16608324]
3. Skopek K, Barbasiewics M, Hampel F, Gladysz JA. Inorg. Chem. 2008; 47:3474–3476. doi: 10.1021/ic702391m. [PubMed: 18380455]
4. Liu Y, Jiang S, Glusac K, Powell DH, Anderson DF, Schanze KS. J. Am. Chem. Soc. 2002; 124:12412–12413. doi: 10.1021/ja027639i. [PubMed: 12381173]
5. Lu W, Mi B-X, Chan MCW, Hui Z, Che C-M, Zhu N, Lee S-T. J. Am. Chem. Soc. 2004; 126:4958–4971. doi: 10.1021/ja0317776. [PubMed: 15080702]
6. Glimsdal E, Dragland I, Carlsson M, Eliasson B, Melo TB, Lindgren M. J. Phys. Chem. A. 2009; 113:3311–3320. doi: 10.1021/jp8083277. [PubMed: 19292436]
7. Camerel F, Ziessel R, Donnio B, Bourgogne C, Guillon D, Schmutz M, Iacovita C, Bucher J-P. Angew. Chem. Int. Ed. 2007; 46:2659–2662. doi: 10.1002/anie.200604012.
8. Schull TL, Kushmerick JG, Patterson CH, George C, Moore MH, Pollack SK, Shashidhar R. J. Am. Chem. Soc. 2003; 125:3202–3203. doi: 10.1021/ja029564o. [PubMed: 12630861]
9. Jude H, Bauer JAK, Connick WB. Inorg. Chem. 2002; 41:2275–2281. doi: 10.1021/ic0108991. [PubMed: 11952385]
10. Jude H, Bauer JAK, Connick WB. Inorg. Chem. 2004; 43:725–733. doi: 10.1021/ic0346329. [PubMed: 14731036]
11. Leung SY-L, Lam WH, Zhu N, Yam VW-W. Organometallics. 2010; 29:5558–5569. doi: 10.1021/om100473q.
12. Wu P-T, Bull T, Kim FS, Luscombe CK, Jenekhe SA. Macromolecules. 2009; 42:671–681. doi: 10.1021/ma8016508.
13. Wang X-Z, Wang Q, Yan L, Wong W-Y, Cheung K-Y, Ng A, Djurisic AB, Chan W-K. Macromol. Rapid Commun. 2010; 31:861–867. doi: 10.1002/marc.200900885. [PubMed: 21590980]
14. Wong W-Y, Ho C-L. Acc. Chem. Res. 2010; 43:1246–1256. doi: 10.1021/ar1000378. [PubMed: 20608673]

15. Rosenberg B, Van Camp L, Krigas T. Nature. 1965; 205:698–699. doi: 10.1038/205698a0. [PubMed: 14287410]
16. Rosenberg B, Van Camp L, Trosko JE, Mansour VH. Nature. 1969; 222:385–386. doi: 10.1038/222385a0. [PubMed: 5782119]
17. Kalinowska-Li U, Ochocki J, Matlawska-Wasowska K. Coord. Chem. Rev. 2008; 252:1328–1345. doi: 10.1016/j.ccr.2007.07.015.
18. Wong E, Giandomenico CM. Chem. Rev. 1999; 99:2451–2466. doi: 10.1021/cr980420v. [PubMed: 11749486]
19. Wheate NJ, Collins JG. Coord. Chem. Rev. 2003; 241:133–145. doi: 10.1016/S0010-8545(03)00050-X.
20. Rajput J, Moss JR, Hutton AT, Hendricks DT, Arendse CE, Imrie C. J. Organomet. Chem. 2004; 689:1553–1568. doi: 10.1016/j.jorganchem.2004.01.034.
21. Liu H-K, Sadler PJ. Acc. Chem. Res. 2011; 44:349–359. doi: 10.1021/ar100140e. [PubMed: 21446672]
22. Wang AH, Nathans J, van der Marel G, van Boom JH, Rich A. Nature. 1978; 276:471–474. doi: 10.1038/276471a0. [PubMed: 723928]
23. Baruah H, Barry CG, Bierbach U. Curr. Top. Med. Chem. 2004; 4:1537–1549. doi: 10.2174/1568026043387313. [PubMed: 15579095]
24. Ma Z, Choudhury JR, Wright MW, Day CS, Saluta G, Kucera GL, Bierbach U. J. Med. Chem. 2008; 51:7574–7580. doi: 10.1021/jm800900g. [PubMed: 19012390]
25. Osa T, Hino H, Fujieda S, Shiio T, Kono T. Chem. Pharm. Bull. 1986; 34:3563–3572. doi: 10.1248/cpb.34.3563. [PubMed: 3815589]
26. Florea A-M, Büsselberg D. Cancers. 2011; 3:1351–1371. doi: 10.3390/cancers3011351. [PubMed: 24212665]
27. Garbutcheon-Singh KB, Myers S, Harper BWJ, Ng NS, Dong Q, Xie C, Aldrich-Wright JR. Metallomics. 2013; 5:1061–1067. doi: 10.1039/c3mt00023k. [PubMed: 23784536]
28. Schertl S, Hartmann RW, Batzl-Hartmann C, Bernhardt G, Spruss T, Beckenlehner K, Koch M, Krauser R, Schlemmer R, Gust R, Schonenberger H. Arch. Pharm. Pharm. Med. Chem. 2004; 337:349–359. doi: 10.1002/ardp.200300856.
29. Gust R, Schonenberger H. Eur. J. Med. Chem. 1993; 28:103–115. doi: 10.1002/ardp.19953280706.
30. Gust R, Schonenberger H. Eur. J. Med. Chem. 1993; 28:117–127. doi: 10.1016/0223-5234(93)90004-X.
31. Schertl S, Hartmann RW, Batzl-Hartmann C, Bernhardt G, Spruss T, Beckenlehner K, Koch M, Krauser R, Schlemmer R, Gust R, Schonenberger H. Arch. Pharm. Pharm. Med. Chem. 2004; 337:335–348. doi: 10.1002/ardp.200300855.
32. Lippard SJ. Pure Appl. Chem. 1987; 59:731–742. doi: 10.1351/pac198759060731.
33. Lippard, SJ.; Bertini, I.; Gray, HB.; Lippard, SJ.; Valentine, JS., editors. Bioinorganic Chemistry. University Sci. Books; Mill Valley: 1994. p. 519-583.
34. Siegel, A.; Siegel, H.; Bloemink, MJ.; Reedijk, J.; Whitehead, JP.; Lippard, SJ., editors. Metal Ions in Biological Systems. Vol. 32. Marcel Dekker Inc.; New York, Basel, Hong Kong: 1996. p. 641p. 687
35. Park GY, Wilson JJ, Song Y, Lippard SJ. Proc. Natl. Acad. Sci. USA. 2012; 109:11987–11992. doi: 10.1073/pnas.1207670109. [PubMed: 22773807]
36. Hollis LS, Amundsen AR, Stern EW. J. Med. Chem. 1989; 32:128–136. doi: 10.1021/jm00121a024. [PubMed: 2909724]
37. Lovejoy KS, Serova M, Bieche I, Emami S, D'Incalci M, Broggini M, Erba E, Gespach C, Cvitkovic E, Faivre S, Raymond E, Lippard SJ. Mol. Cancer Ther. 2011; 10:1709–1719. doi: 10.1158/1535-7163.MCT-11-0250. [PubMed: 21750216]
38. Zhang CX, Lippard SJ. Curr. Opin. Chem. Biol. 2003; 7:481–489. doi: 10.1016/S1367-5931(03)00081-4. [PubMed: 12941423]
39. Kasparkova J, Marini V, Najajreh Y, Gibson D, Brabec V. Biochemistry. 2003; 42:6321–6332. doi: 10.1021/bi0342315. [PubMed: 12755637]
40. APEX2 v2010.7-0 Bruker 2005-2010

41. Nakayama S, Torikoshi Y, Takahashi T, Yoshida T, Sudo T, Matsushima T, Kawasaki Y, Katayama A, Gohda K, Hortobagyi GN, Noguchi S, Sakai T, Ishihara H, Ueno NT. Breast Cancer Res. 2009; 11:R12. doi: 10.1186/bcr2231. [PubMed: 19239702]
42. Wagner JM, Karnitz LM. Mol. Pharmacol. 2009; 76:208–214. doi: 10.1124/mol.109.055178. [PubMed: 19403702]
43. Andriani F, Perego P, Carenini N, Sozzi G, Roz L. Neoplasia. 2006; 8:9–17. doi: 10.1593/neo.05517. [PubMed: 16533421]
44. Potapinska O, Zawadzka-Krajewska A, Kotula I, Pyrzak B, Gomulka K, Wasik M, Demkow U. Folia Histochem. Cytobiol. 2009; 47:647–651. doi: 10.2478/v10042-009-0119-7. [PubMed: 20430734]
45. Schutte B, Nuydens R, Geerts H, Ramaekers F. J. Neurosci. Methods. 1998; 86:63–69. doi: 10.1016/S0165-0270(98)00147-2. [PubMed: 9894786]
46. van Engeland M, Nieland LJW, Ramaekers FCS, Schutte B, Reutelingsperger CPM. Cytometry. 1998; 31:1–9. doi: 10.1002/(SICI)1097-0320(19980101)31:1<1::AIDCYTO1>3.0.CO;2-R. [PubMed: 9450519]
47. Cyr L, Langler R, Lavigne C. Anticancer Res. 2008; 28:2753–2764. [PubMed: 19035306]
48. Vermes I, Haanen C, Steffens-Nakken H, Reutelingsperger C. J. Immunol. Methods. 1995; 184:39–51. doi: 10.1016/0022-1759(95)00072-I. [PubMed: 7622868]
49. Robles-Escajeda E, Lerma D, Nyakeriga AM, Ross JA, Kirken RA, Aguilera RJ, Varela-Ramirez A. PLoS ONE. 2013; 8:e73508. doi: 10.1371%2Fjournal.pone.0073508. [PubMed: 24039967]
50. Cao X-C, Zhang W-R, Cao W-F, Liu B-W, Zhang F, Zhao H-M, Mang R, Zhang L, Niu R-F, Hao X-S, Zhang B. PLoS ONE. 2013; 8:e56735. doi: 10.1371/journal.pone.0056735. [PubMed: 23468877]
51. Rossen NS, Hansen AJ, Selhuber-Unkel C, Oddershede LB. PLoS ONE. 2011; 6:e25196. doi: 10.1371/journal.pone.0025196. [PubMed: 21966453]
52. Keyhani J, Jafari-Far F, Einollahi N, Ghadirian E, Keyhani E. Immunol. Lett. 1998; 62:81–86. doi: 10.1016/S0165-2478(98)00019-4. [PubMed: 9698102]
53. Hohenberg P, Kohn W. Phys. Rev. 1964; 136:B864–B871. doi: 10.1103/PhysRev.136.B864.
54. Parr, RG.; Yang, W., editors. Density-Functional Theory of Atoms and Molecules. Oxford University Press; Oxford: 1989.
55. Becke AD. Phys. Rev. A. 1988; 38:3098–3100. doi: 10.1103/PhysRevA.38.3098. [PubMed: 9900728]
56. Becke AD. J. Chem. Phys. 1993; 98:1372–1378. doi: 10.1063/1.464304.
57. Becke AD. J. Chem. Phys. 1993; 98:5648–5653. doi: 10.1063/1.464913.
58. Lee CT, Yang WT, Parr RG. Phys. Rev. B. 1988; 37:785–789. doi: 10.1103/PhysRevB.37.785.
59. Frisch, MJ.; Trucks, GW.; Schlegel, HB.; Scuseria, GE.; Robb, MA.; Cheeseman, JR.; Scalmanai, G.; Barone, V.; Mennucci, B.; Petersson, GA.; Nakatsuji, H.; Caricato, M.; Li, X.; Hratchian, HP.; Izmaylov, AF.; Bloino, J.; Zheng, G.; Sonnenberg, JL.; Hada, M.; Ehara, M.; Toyota, K.; Fukuda, R.; Hasegawa, J.; Ishida, M.; Nakajima, T.; Honda, Y.; Kitao, O.; Nakai, H.; Vreven, T.; Montgomery, JA., Jr.; Peralta, JE.; Ogliaro, F.; Bearpark, M.; Heyd, JJ.; Brothers, E.; Kudin, KN.; Staroverov, VN.; Kobayashi, R.; Normand, J.; Raghavachari, K.; Rendell, A.; Burant, JC.; Iyengar, SS.; Tomasi, J.; Cossi, M.; Rega, N.; Millam, NJ.; Klene, M.; Knox, JE.; Cross, JB.; Bakken, V.; Adamo, C.; Jaramillo, J.; Gomperts, R.; Stratmann, RE.; Yazyev, O.; Austin, AJ.; Cammi, R.; Pomelli, C.; Ochterski, JW.; Martin, RL.; Morokuma, K.; Zakrzewski, VG.; Voth, GA.; Salvador, P.; Dannenberg, JJ.; Dapprich, S.; Daniels, AD.; Farkas, Ö .; Foresman, JB.; Ortiz, JV.; Cioslowski, J.; Fox, DJ. Gaussian 09, Revision D.01. Gaussian, Inc.; Wallingford CT: 2009.
60. Dunning, TH.; Hay, PJ.; Schaefer, HF., III, editors. Modern Theoretical Chemistry. 3. Methods of Electronic Structure Theory. Plenum Press; New York: 1977. p. 1-28.
61. Wadt WR, Hay PJ. J. Chem. Phys. 1985; 82:270–283. doi: 10.1063/1.448799.
62. Wadt WR, Hay PJ. J. Chem. Phys. 1985; 82:299–310. doi: 10.1063/1.448975.
63. Peng C, Schlegel HB. Israel J. of Chem. 1993; 33:449–454.
64. Peng C, Ayala PY, Schlegel HB, Frisch MJ. J. Comp. Chem. 1996; 17:49–56. doi: 10.1002/(SICI)1096-987X(19960115)17:1<49::AID-JCC5>3.0.CO;2-0.

65. Tomasi J, Mennucci B, Cammi B. Chem. Rev. 2005; 105:2999–3094. doi: 10.1021/cr9904009. [PubMed: 16092826]
66. Yoshizawa K, Ito A, Tanaka K, Yamabe T. Synth. Met. 1992; 48:271–282. doi: 10.1016/0379-6779(92)90230-G.
67. Bushby RJ, McGill DR, Ng KM, Taylor N. J. Chem. Soc., Perkin Trans. 1997; 2:1405–1414. doi: 10.1039/A605722E.
68. Ito A, Ino H, Tanaka K, Kanemoto K, Kato T. J. Org. Chem. 2002; 67:491–498. doi: 10.1021/jo0160571. [PubMed: 11798322]
69. Yoshizawa K, Chano A, Ito A, Tanaka K, Yamabe T, Fujita H, Yamauchi J. Chem. Lett. 1992:369–372. doi: 10.1246/cl.1992.369.
70. Wienk MM, Janssen RAJ. Chem. Commun. 1996:267–268. doi: 10.1039/CC9960000267.
71. Wienk MM, Janssen RAJ. J. Am. Chem. Soc. 1997; 119:4492–4501. doi: 10.1021/ja963772x.
72. Ito A, Ota K-I, Tanaka K, Yanabe T, Yoshizawa Y. Macromolecules. 1995; 28:5618–5625. doi: 10.1021/ma00120a029.
73. Sadighi JP, Singer RA, Buchwald SL. J. Am. Chem. Soc. 1998; 120:4960–4976. doi: 10.1021/ja980052c.
74. Jamart-Gregoire B, Leger C, Caubere P. Tetrahedron Lett. 1990; 31:7599–7602. doi: 10.1016/S0040-4039(00)97309-X.
75. Ng PL, Lambert JN. Synlett. 1999:1749–1750. doi: 10.1055/s-1999-2923.
76. Bohm S, Oriana S, Spatti G, Di Re F, Breasciani G, Pirovano C, Grosso I, Martini C, Caraceni A, Pilotti S, Zunino F. Oncology. 1999; 57:115–120. doi: 10.1159/000012017. [PubMed: 10461057]
77. Hickman JA. Cancer Metastasis Rev. 1992; 2:121–139. doi: 10.1007/BF00048059. [PubMed: 1327566]
78. Ding H, Han C, Zhu J, Chen CS, D'Ambrosio SM. Int. J. Cancer. 2005; 113:803–810. doi: 10.1002/ijc.20639. [PubMed: 15499625]
79. Hynes RO. Cell. 1992; 69:11–25. doi: 10.1016/0092-8674(92)90115-S. [PubMed: 1555235]
80. Lauffenburger DA, Horwitz AF. Cell. 1996; 84:359–369. doi: 10.1016/S0092-8674(00)81280-5. [PubMed: 8608589]
81. Kasibhatla S, Brunner T, Genestier L, Echeverri F, Mahboubi A, Green DR. Mol. Cell. 1998; 1:543–551. doi: 10.1016/S1097-2765(00)80054-4. [PubMed: 9660938]
82. Wilson JJ, Lippard SJ. J. Med. Chem. 2012; 55:5326–5336. doi: 10.1021/jm3002857. [PubMed: 22606945]

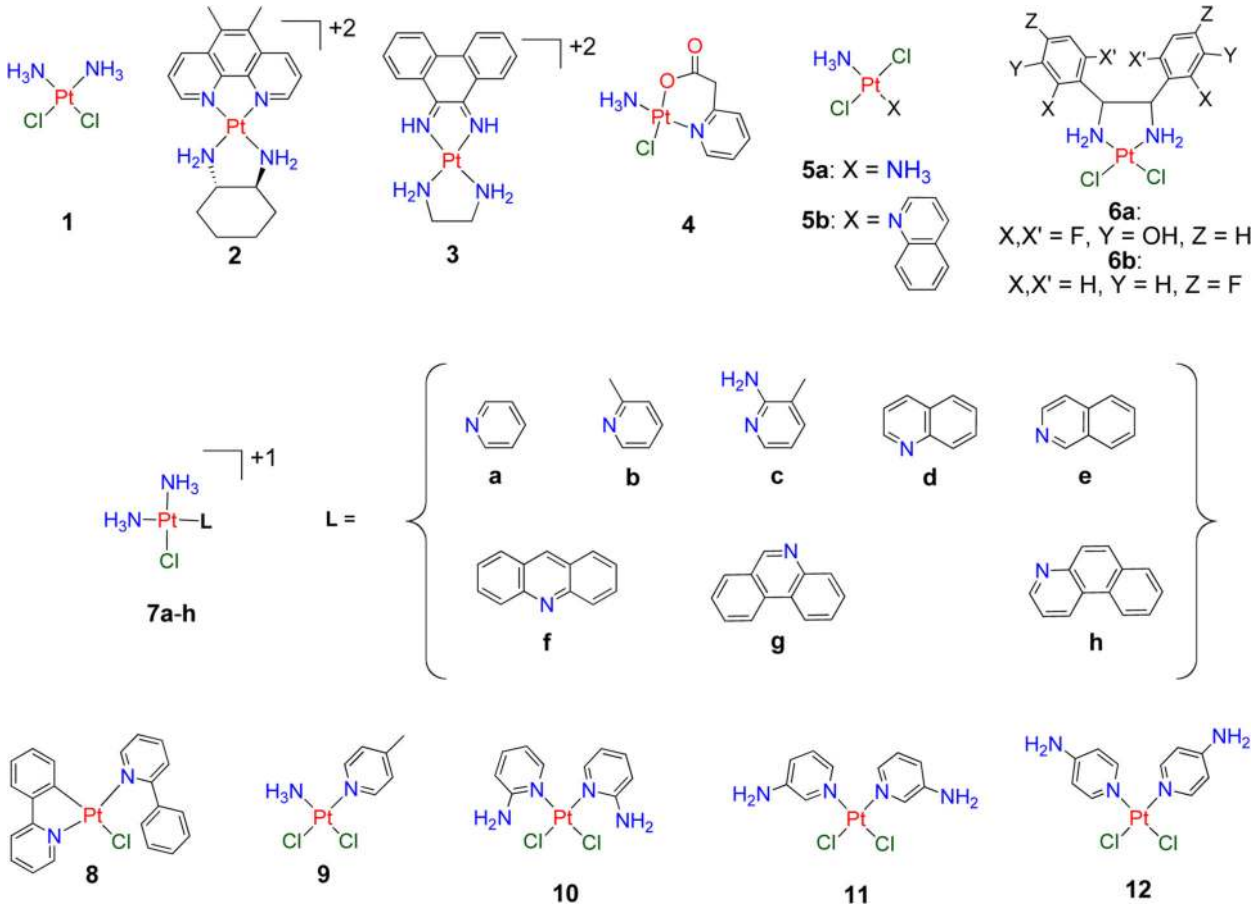

Fig. 1.
Structures of explored anti-tumor platinum complexes [15–39].

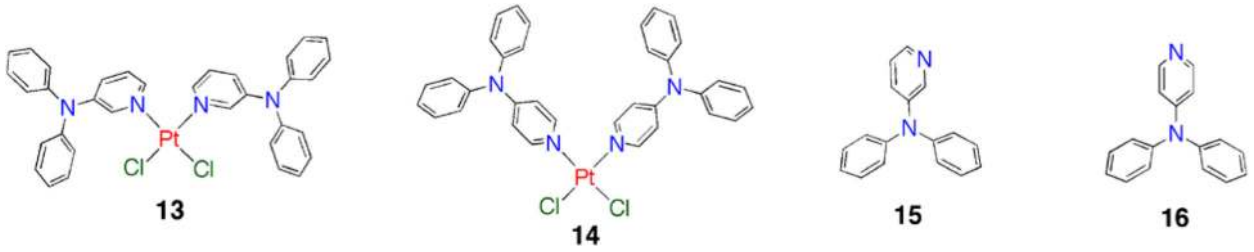

Fig. 2.
Meta- and *para*- Pt(II) complexes and pyridineamine ligands.

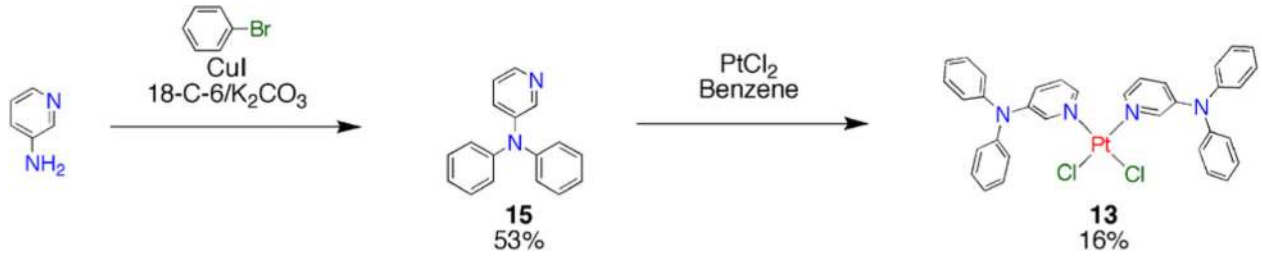

Scheme 1.

Synthesis of *meta*- ligand **15** and *cis*- complex **13** [66-73].

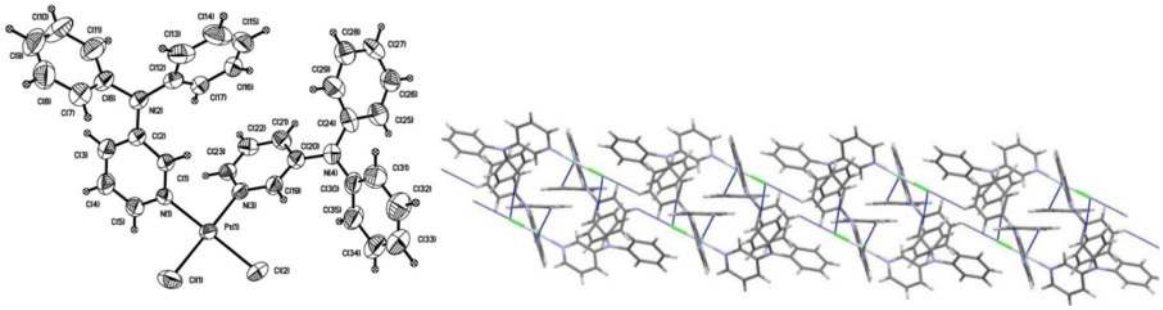

Fig. 3.
Molecular structure of **13** and the H···Cl interactions that generate the 2-D structure.

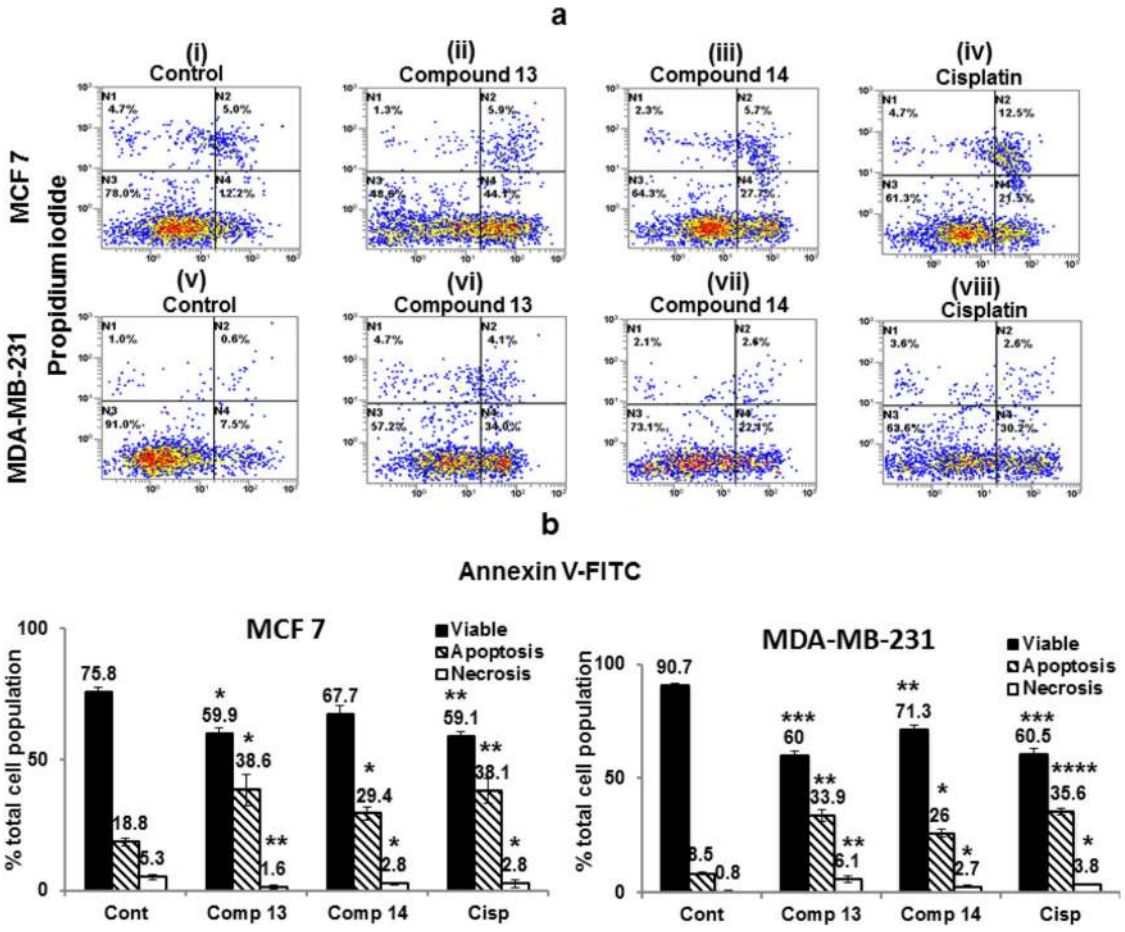

Fig. 4.

Compounds **13** and **14** induced PS translocation in plasma membranes of breast cancer cells. Compounds **13**, **14**, and cisplatin were added to the culture medium at their respective IC_{50} concentrations, incubated for 24 h, stained with Annexin V-FITC/PI and analyzed by flow cytometry as described in the Experimental Section. Panel a: Flow cytogram of Pt compounds-treated MCF 7 and MDA-MB-231 cells. MCF 7 (Panel a, i–iv) and MDA-MB-231 (Panel a, v–viii) cells were treated with the Pt complexes at their IC_{50} concentrations followed by staining with Annexin V-FITC and PI; samples were then sorted by flow cytometry as described in the Experimental Section. The experiments were carried out in triplicate and repeated 3–4 times, but data shown here are from a single experiment. The lower-left quadrant shows control cells that are negative to Annexin V and PI; the lower-right quadrant represents early apoptotic cells, which are Annexin V-positive and PI-negative; the upper-right quadrant shows Annexin V-positive and PI-positive late-apoptotic cells and the upper-left quadrant demonstrates Annexin V-negative and PI-positive necrotic cells. Panel b: The percentages of viable, apoptotic, and necrotic cells were determined from the relative intensities of the Annexin V and PI staining. The results shown are mean ± SD (n = 3), indicating a significant difference from the control (DMSO-treated) group (*, $P \leq 0.05$; **, $P \leq 0.01$; ***, $P \leq 0.001$; ****, $P \leq 0.0001$) as determined by the student's *t*-test.

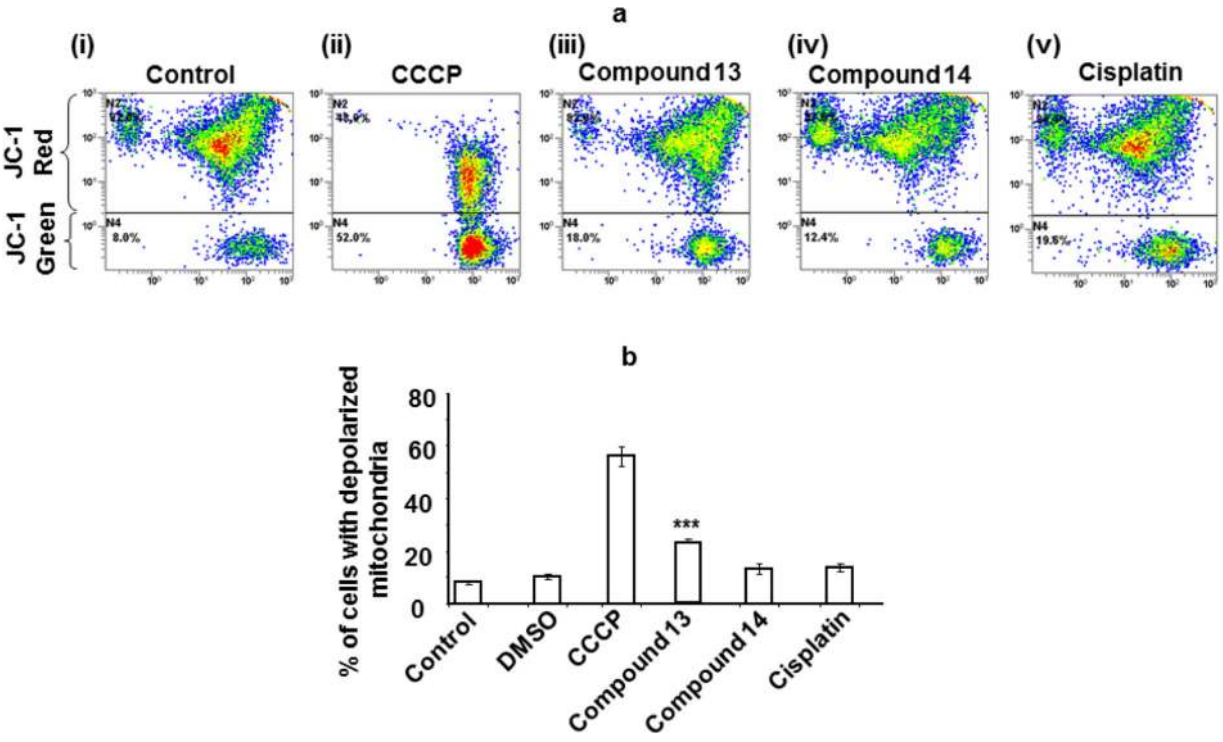

Fig. 5.

Compound **13** depolarizes mitochondrial membranes in MDA-MB-231 cells. Cells were treated with the Pt complexes for 8 h and the changes in ΔΨm were determined by staining with lipophilic fluorophore JC-1 dye followed by flow-cytometric analysis. In Panel a, representative flow cytometric dot plots (i–v) used to quantify the distribution of cells emitting green signal, due to depolarized mitochondria (lower section on the plots). The color of dots (events) on the plots shows a density gradient transitioning from blue (low) to red (high) gradient. CCCP (50 μM) was used as a positive control to assess the mitochondrial ΔΨm. Approximately 10,000 events were acquired and analyzed. Panel b (bar graph) represents the results of mitochondria membrane depolarization that were obtained from the flow cytograms shown in Panel a. Results shown are the mean of three independent measurements. Analysis using the two-tailed student's paired *t*-test comparing compound **13**-treated cells with DMSO-solvent controls gave $P < 0.001$ (***).

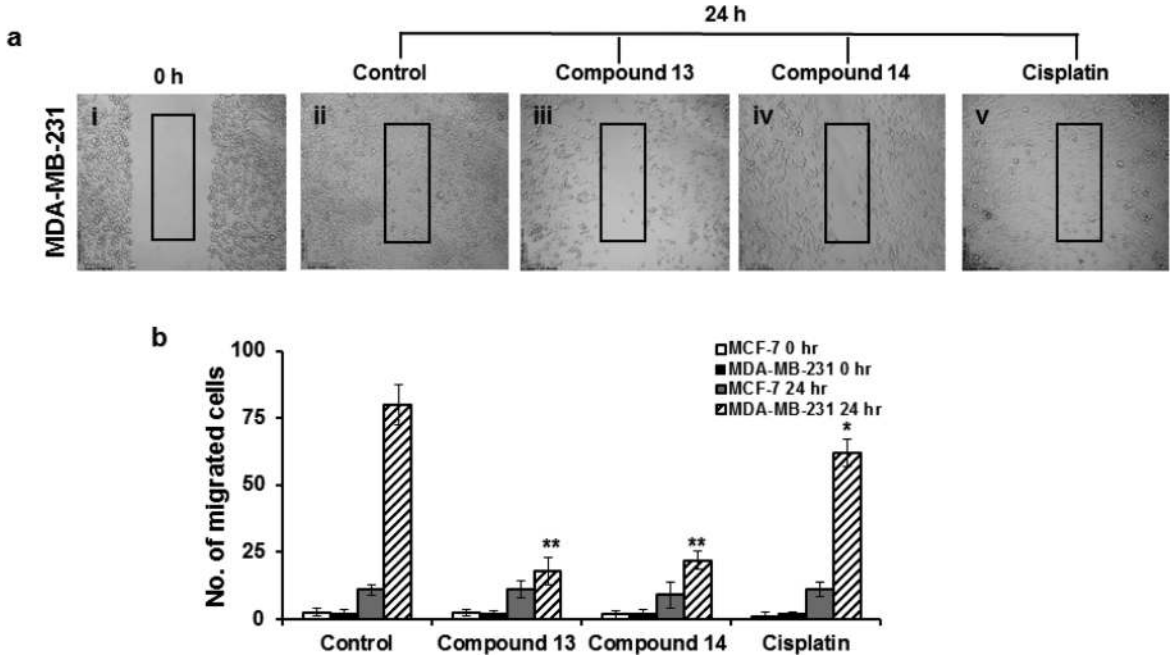

Fig. 6.

Compounds **13** and **14** inhibit the migration of MDA-MB-231 cells. The monolayer of MCF 7 and MDA-MB-231 was scratch-wounded using a 10 μm pipette tip, and treated for 24 h with compound **13**, **14**, and cisplatin with their IC_{50} concentrations. The photographs were captured at 0 h and 24 h time points as indicated in each photograph. Photograph i: MDA-MB-231 at 0 h wound-scratch; photograph ii: 24 h; photograph iii: compound **13**, 24 h; photograph iv: compound **14**, 24 h; photograph v: cisplatin, 24 h. The cells that migrated into the wound region were counted and are represented in Fig. 6b and compared with non-migratory MCF 7 cells. The data shown here are the mean (± SE) of three independent experiments. * $P < 0.01$, ** $P < 0.001$.

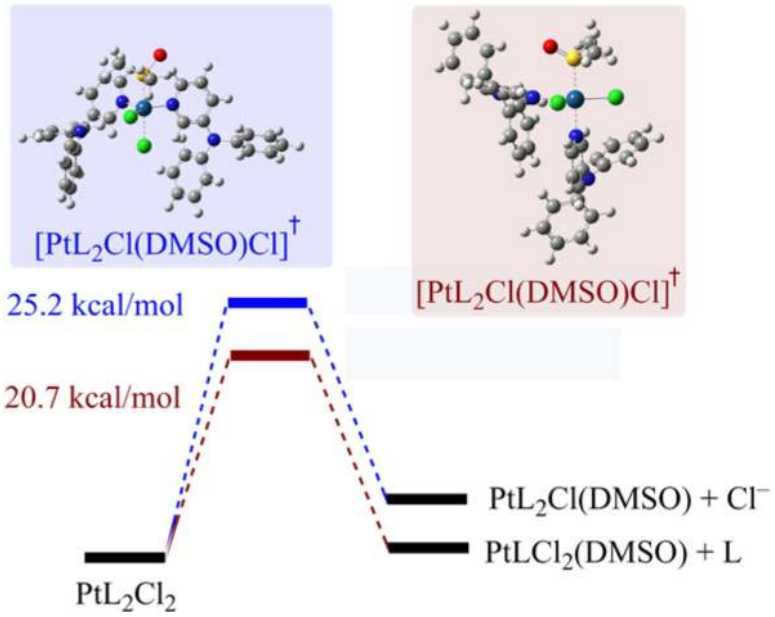

Fig. 7.

Potential energy surface diagram of the SN2 mechanism proposed for substitution of the pyrdineamine ligand (L) (red curve) by a DMSO molecule and comparison with the competing substitution reaction for removal of the chloride anion (blue curve).

Table 1

Principal Crystallographic Parameters for Complex 13.[a]

Empirical Formula	**$C_{34}H_{28}Cl_2N_4Pt$ (13)**
Formula Weight	758.59
Crystal System	Monoclinic
Space Group	$P2_1/c$
Unit Cell Dimensions	
A (Å)	11.8785(5)
B (Å)	14.3488(6)
c (Å)	20.2958(7)
B (°)	116.587(2)
Volume (Å^3)	3093.5(2)
Z	4
Total Reflections	38529
Independent Reflections	7458
Completeness to Θ(%)	28(99.9)
R1 [I>2sigma(I)]	0.0191
wR2 [I>2sigma(I)]	0.0690

[a]Crystals grown from dichloromethane at 25 °C.

Table 2

Selected Bond Lenghts (Å).

	meta-cis (**13**)[a]
Pt-Cl	2.295(1), 2.296(1)
Pt-N	2.027(3), 2.033(3)
N1-C1	1.337(4), 1.342(4)
N1-C5	1.347(4), 1.349(4)
N2-C2	1.398(4), 1.396(4)
N2-C6	1.412(5), 1.425(5)
N2-C12	1.436(4), 1.436(5)

[a]The two values correspond to each of the two asymmetrical ligands.

Table 3

Cell viability and cytotoxicity assay.

Cells	Compound 13 IC_{50} (μM) ± SD	Compound 14 IC_{50} (μM) ± SD	Cisplatin IC_{50} (μM) ± SD
MCF 7	1 ± 0.4	1 ± 0.2	5 ± 0.7
MDA-MB-231	7.5 ± 1.3	1 ± 0.3	10 ± 1.1

IC_{50} half-maximal cytotoxic concentrations, SD standard deviation, ± values are the estimated IC_{50} interval.